

DEVELOPMENT OF UCAV AERODYNAMICS IN UTM

Khushairi Amri Kasim, Shabudin Mat *, Shuhaimi Mansor
Faculty of Mechanical Engineering, Universiti Teknologi Malaysia,
81310 UTM Johor Bahru, Johor, Malaysia.

* Corresponding author: shabudin@utm.my

ABSTRACT

The rapid development and advancement in unmanned aerial vehicle/unmanned combat aerial vehicle (UAV/UCAV) has triggered the increasing interest in development of UAV/UCAV. Numerous of the research performed experimentally and numerically in order to have better understanding on the complicated flow behavior above low sweep blended delta wing design which commonly used in UCAV configuration. NATO RTO AVT-161 is one of the pioneer research programmes in the UCAV configuration throughout generic model SACCON. However, the current knowledge on the SACCON configuration is very limited to certain angle of attacks and flow conditions such Reynold number. This current research will highlight the aerodynamics and flow characteristics of the SACCON at Reynolds number of 0.51×10^6 and 0.78×10^6 towards different angle of attacks. A semi-span wind tunnel model was designed and fabricated with the capability to install pressure taps on several positions inside the model. The experiments were conducted in a closed-circuit low speed wind tunnel at speeds of 17 and 26 m/s that corresponding to 0.51×10^6 and 0.78×10^6 Reynolds numbers based on model mean aerodynamic chord, respectively. The angles of attack were varied from -10° to 30° . During the experiment, two measurement techniques were employed on the wing, which were the steady balance measurement and surface pressure measurement. The findings highlight the effects of Reynolds number toward aerodynamic coefficients and pressure distribution above the wing. The experimental data conclude that the aerodynamic characteristics of SACCON wing is influenced by flow structure above the wing. The SACCON wing exhibits three major vortex structures which are apex vortex, thickness vortex and tip vortex. Additional suction peak is observed near the trailing edge downstream from wing at higher angle of attack suggesting possibility of another vortex structure developed. The current findings may contribute to a better understanding of flow physics on UCAV configuration.

KEYWORD

SACCON wing, Wind Tunnel Testing, Reynolds numbers

INTRODUCTION

Throughout the years, there have been rapid development on the unmanned aerial vehicle/unmanned combat aerial vehicle (UAV/UCAV) around the world due their prevalent applications in civil and military sectors (Rogalski, 2020). UAV/UCAV or unmanned aircraft is an air vehicle without pilot onboard and can be remotely controlled or autonomously. This development had raised the improvement in wide scale application regarding unmanned aircraft such in monitoring, surveying, inspection and emergency response (Nawawi, 2021). Considering the flexibility in operation and wide area coverage, unmanned aircraft is more favourable compared to the ground approaches (Jusoh, 2021). Aside from high mobility, the employment of unmanned aircraft also reduces the operational cost as well as prevent any casualties toward the operators (Li, 2020; Kováčik, 2020; Skjervold, 2018). For UCAV, their function is not limited only to reconnaissance, surveillance and intelligence mission. UCAV commonly equipped with aircraft ordnance such bombs, missiles and rockets for airstrike mission (Chamola, 2021).

The advancement of the technology has triggered essential of UCAV that capable of higher speed and manoeuvre alongside with specific mission requirement. Thus, delta wing concept was introduced in UCAV development to achieve required conditions. Most of the current and future UAV/UCAV configurations are using delta wing planform with low to medium sweep angle i.e., 35° to 55° (Gursul,

2005; Gordnier, 2003). This is due to the considerations of the performance and endurance of the real flight (Schütte, 20212). The delta wing design is having aerodynamic advantages and higher power efficiency compared to the conventional wing which enable operation at near and post stall regimes for extra aerodynamic lift. The extra lift generated from the leading-edge vortex improve overall lift generation on the wing and beneficial at lower angles of attack condition (Maqsood, 2015). The most common planform used in current and future delta-winged UCAV are diamond and lambda wing as shown in Figure 1. The lambda wing planform features a cranked design at the trailing edge meanwhile diamond wing incorporated extended trapezoidal trailing edge. The delta-winged UCAV design commonly incorporated blended wing design to produce higher volume for larger payloads and system/equipment integrations. The blended wing design introduce inconsistent leading-edge radius from the apex of the wing toward trailing edge which induced complicated vortical flow above the wing. The attached flow region near the apex will influenced the formation of leading-edge vortex downstream depending on the flow conditions i.e., angle of attack, Reynolds number and leading-edge profile (Tajuddin, 2020).

Throughout the world, numerous manufacturers are working and developing UCAV design configuration for current and future uses. There are several aircraft UCAVs available and are operating as shown in Figure 2. Most of the UCAV design incorporated with the lambda wing planform with highly blended wing design. This is mainly due to the stealth requirements priority (Sepulveda, 2017). Air forces and defence companies are currently investing in long term development of sixth-generation fighter aircraft to be employed in service by year of 2035-2040 (Jordan, 2021). The sixth-generation fighter aircraft will be incorporated with the unmanned features. Several such ongoing projects are BAE Systems Tempest (Europe), F/A-XX (United States) and Mikoyan PAK DP (Russia). However, to develop the agile and highly swept UCAV configuration is very demanding endeavour. The essential performance and manoeuvrability requirement from the UCAV design required tremendous, detailed data such aerodynamic performance at extensive flight conditions, mass distribution, system integration and propulsion performance (Liersch, 2020). At times, the UCAV design and development is compromised between high-speed flight performance and manoeuvrability at low-speed flight (Nangia, 2016).

Due to rapid advancement in UCAV development, there has been increasing interest in understanding the flow characteristics on non-slender delta wing used in UCAV configurations. Numerous of studies were performed to understand the flow behaviour around the low sweep blended delta wings through the experiments and to provide validation data for evaluation of the major CFD codes. The first program on UCAV configuration was organised by The Technical Cooperation Program (TTCP). The program was focussing on the 1303 UCAV configuration. NATO Research and Technology Organization (RTO) task group established their UCAV configuration program under applied vehicle technology (AVT) entitled "Assessment of Stability and Control Prediction Methods for NATO Air & Sea Vehicles

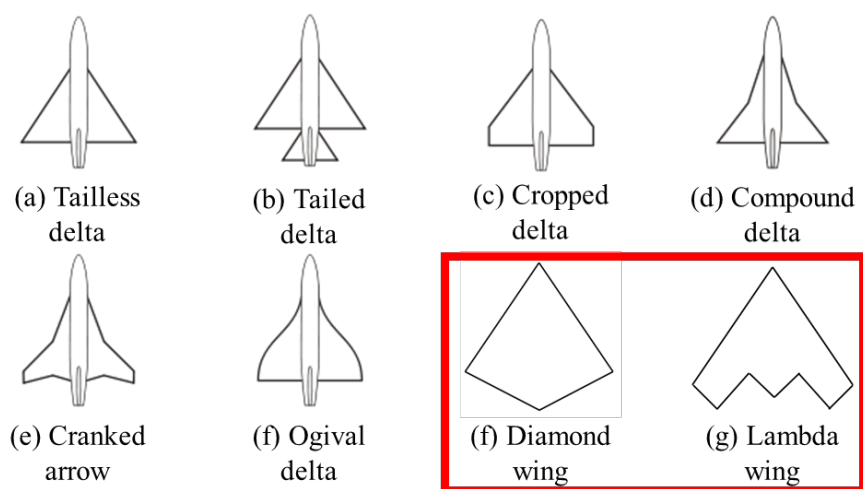


Figure 1: Types of delta wing used in aircraft and UAV/UCAV

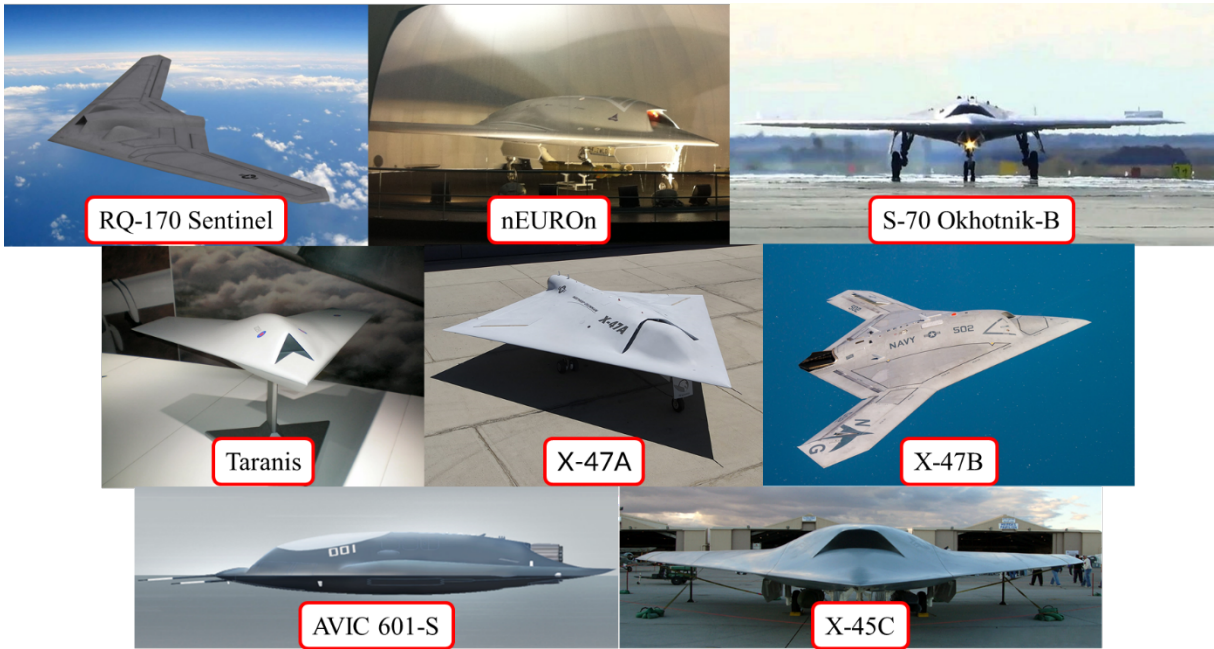


Figure 2: Current and future UCAV design used in aircraft

METHODOLOGY

A semi-span model was designed and fabricated in UTM Aerolab that replicates the original SACCON from AVT-161. The design and dimension of the model is based on the model used within AVT-161 programme. The model was designed to have semi-span model to accommodate the availability test section size without compromising the model dimension. The stand-off for the model was designed based on the fuselage profile and dimension. Figure 3 shows the UTM-SACCON wind tunnel model specification and dimension. To measure the pressure on the upper surface of the wing, the model has been installed with 99 pressure taps with diameter of 1 mm located on the entire wing. The pressure taps are connected to the pressure scanner through the vinyl tube.

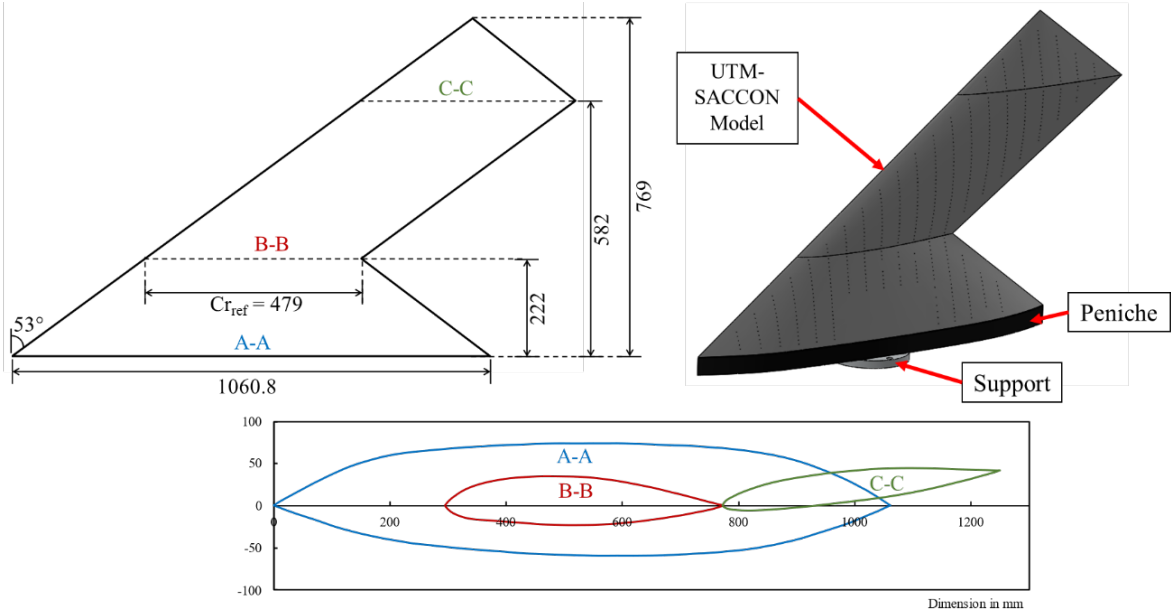


Figure 3: TM-SACCON configuration dimension and geometrical properties

The experiments were performed in the UTM Aerolab wind tunnel. The size of the test section is $2\text{m} \times 1.5\text{m} \times 5\text{m}$ with capability of 80 m/s maximum speed. The installation of the model in the test section is shown in Figure 4 with notation of forces and moments. F_x , F_y and F_z represent the direction of drag, lift and side force of the model while M_z represent the model pitching moment. The model is attached to 6-component external balance JR3 160M50 located underneath the test section. The UTM-SACCON wind tunnel model was mounted above additional stand-off (*peniche*) to avoid the flow interactions between wind tunnel boundary layer with the model.

The experiments were performed at the speeds of 17 and 26 m/s that corresponding to 0.51×10^6 and 0.78×10^6 Reynolds number based on reference chord of 0.479 meter. The angles of attack were varied from -10° to 30° by controlling the wind tunnel turntable automatically. In this study, two measurement techniques were employed on the wing. The first measurement technique was the steady balance data while the final one was the surface pressures measurement. All forces and moments in x , y and z have been recorded at three times sampling and repeatability process had been considered. The measured force in the y and x directions were normalized into the lift and drag coefficients (C_L & C_D) of the model while the moment in z direction is converted into the wing pitching moment coefficient (C_M). The uncertainty analysis was performed for all forces and moments channel. The standard error was then calculated separately for these forces and moments channel at each angle of attack. The maximum uncertainty of data for all forces and moments channel is at 0.6% . The pressure measurement on the surface was obtained at measurement planes of 0.1 to 0.9 . The pressure distribution on plane 0.4 to 0.6 is limited in the fuselage section is due to restriction in the model cavity (placement of the wing support to the tunnel). The surface pressure measurement was recorded using the FKPS 30DP electronic pressure scanner with an accuracy of ± 1 psi. The measured pressures then were converted into pressure coefficients (C_p). Only selected angle of attack for pressure distribution above the wing is presented within this paper. Table 2 shows the experiment conditions in this paper.

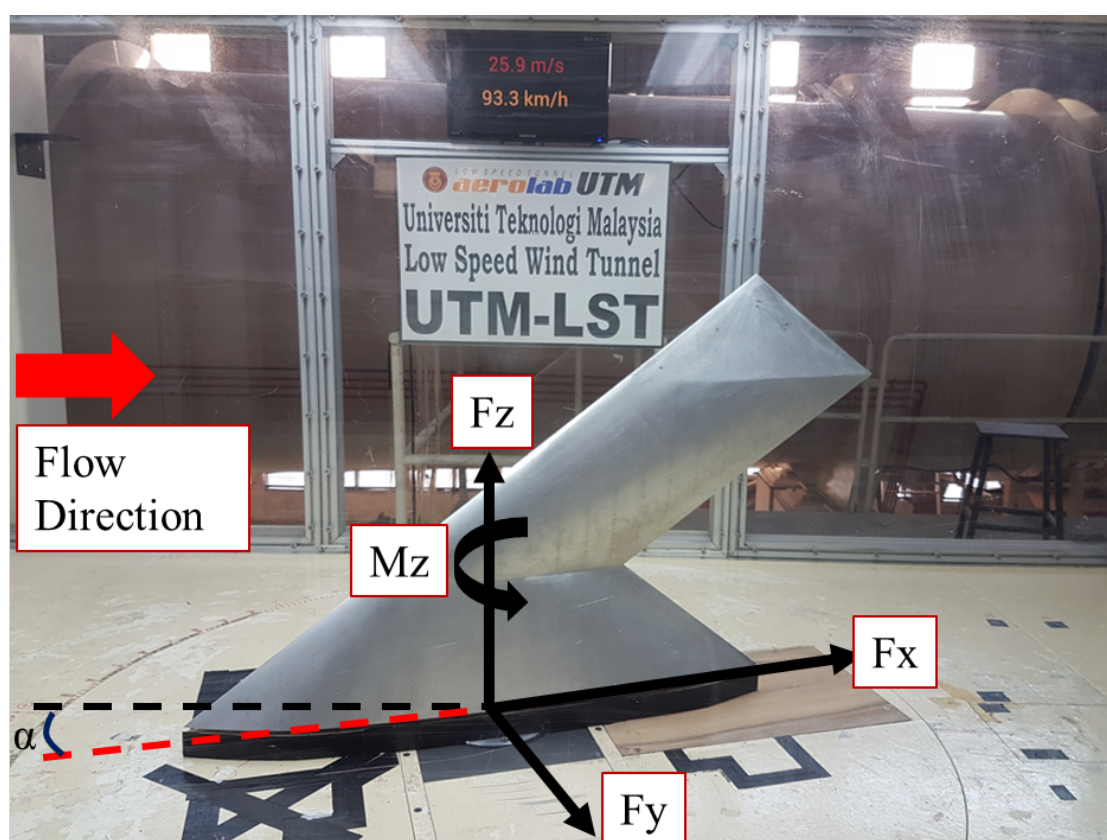


Figure 4: Installation of UTM-SACCON with forces and moment notation

Table 2: Experiment conditions

Parameters	Values
Pressure distribution measurement planes (Y/Cr)	0.1, 0.2, 0.3, 0.4, 0.5, 0.6, 0.7, 0.8, 0.9
Freestream velocity (m/s)	17, 26
Reynolds number (based on reference chord)	0.51×10^6 , 0.78×10^6
Angle of attack, α (°)	-10 to 30 (step: 2)

CONCLUSION

In conclusion, the author can share any engineering-related material on this platform. It is also simple to send the required documents because they all used the Book Antiqua typeface with a size of 10.5 points.

ACKNOWLEDGEMENT

The research has been funded by FRGS 4F718

REFERENCE

Chamola, V., Kotesch, P., Agarwal, A., Naren, Gupta, N., & Guizani, M. (2021). A Comprehensive Review of Unmanned Aerial Vehicle Attacks and Neutralization Techniques. *Ad Hoc Networks*, 111, 1-20.

Gordnier, R. E., & Visbal, M. R. (2003). Higher-order compact difference scheme applied to the simulation of a low sweep delta wing flow. 41st Aerospace Sciences Meeting and Exhibit, 6-9 January 2003, Reno: AIAA 2003-620.

Gursul, I., Gordnier, R., & Visbal, M. (2005). Unsteady aerodynamics of nonslender delta wings. *Progress in Aerospace Sciences*, 41(7), 515-557.

Jordan, J. (2021). The future of unmanned combat aerial vehicles: An analysis using the Three Horizons framework. *Futures*, 134, 1-11.

Jusoh, M. I., Rosmin, N., Mustaamal, A. H., Aripriharta, Hussin, S. M., Amin, M. M., & Ali, N. A. (2021). A Review on Unmanned Aerial Vehicle for High Altitude Visual Inspection. *Journal of Tomography System & Sensors Application*, 4(2), 128-134.

Kováčik, L., & Novák, A. (2020). Comparison of Aerial Application vs. Ground Application. *Transportation Research Procedia*, 44, 264-270.

Li, Y. F., Shi, J. P., Jiang, W., Zhang, W. G., & Lyu, Y. X. (in press 2021). Autonomous maneuver decision-making for a UCAV in short-range aerial combat based on an MS-DDQN algorithm. *Defence Technology*, 1-18. <https://doi.org/10.1016/j.dt.2021.09.014>.

Liersch, C. M., Schutte, A., Siggel, M., & Dornwald, J. (2020). Design studies and multi-disciplinary assessment of agile and highly swept wing configurations. *CEAS Aeronautical Journal*, 11, 781-802.

Maqsood, A., & Go, T.H. (2015). Aerodynamic characteristics of a flexible membrane micro air vehicle. *Aircraft Engineering and Aerospace Technology*, 87(1), 30-37.

Nangia, R., Ghoreyshi, M., van Rooij, M. P. C., & Cummings, R. M. (2019). Aerodynamic design assessment and comparisons of the MULDICON UCAV concept. *Aerospace Science and Technology*, 93, 1-23.

Nawawi, S. W., Ahmed Abdou, A. A. M, & Abd Aziz, N. A. (2021). CNN-based Off-board Computation for Real-time Object Detection and Tracking Using a Drone. *Journal of Tomography System & Sensors Application*, 4(2), 11-20.

Rogalski, T., Rzucidło, P., & Prusik, J. (2020). Unmanned aircraft automatic flight control algorithm in a spin maneuver. *Aircraft Engineering and Aerospace Technology*, 92(8), 1215-1224.

Schütte, A., Hummel, D., & Hitzel, S. M. (2012). Flow physics analyses of a generic unmanned combat aerial vehicle configuration. *Journal of Aircraft*, 49(6), 1638-1651.

Sepulveda, E., & Smith, H. (2017). Technology challenges of stealth unmanned combat aerial vehicles. *The Aeronautical Journal*, 121(1243), 1261-1295.

Skjervold, E., & Hoelsreter, φ. T. (2018). Autonomous, Cooperative UAV Operations Using COTS Consumer Drones and Custom Ground Control Station. *MILCOM 2018 - 2018 IEEE Military Communications Conference (MILCOM)*, 29-31 October 2018, Los Angeles: IEEE.

Tajuddin, N., Mat, S., & Said, M. (2020). Tomography Systems and Sensor Applications Flow Visualization Above Blunt-Edged Delta Wing. *Journal of Tomography System & Sensors Application*, 3(1), 86-97.